

Leading chiral three-nucleon forces along isotope chains in the calcium region

V. Somà,^{1,2,*} A. Cipollone,³ C. Barbieri,^{3,†} P. Navrátil,⁴ and T. Duguet^{5,6,‡}

¹*Institut für Kernphysik, Technische Universität Darmstadt, 64289 Darmstadt, Germany*

²*ExtreMe Matter Institute EMMI, GSI Helmholtzzentrum für Schwerionenforschung GmbH, 64291 Darmstadt, Germany*

³*Department of Physics, University of Surrey, Guildford GU2 7XH, UK*

⁴*TRIUMF, 4004 Westbrook Mall, Vancouver, BC, V6T 2A3, Canada*

⁵*CEA-Saclay, IRFU/Service de Physique Nucléaire, 91191 Gif-sur-Yvette, France*

⁶*National Superconducting Cyclotron Laboratory and Department of Physics and Astronomy, Michigan State University, East Lansing, MI 48824, USA*

(Dated: March 28, 2014)

Three-nucleon forces (3NFs), and in particular terms of the Fujita-Miyazawa type, strongly influence the structure of neutron-rich exotic isotopes. Ab initio calculations have shown that chiral two- and three-nucleon interactions correctly reproduce binding energy systematics and neutron driplines of oxygen and nearby isotopes. Exploiting the novel Gorkov-Green's function approach, we present the first ab initio investigation of Ar, K, Ca, Sc and Ti isotopic chains. Leading chiral 3N interactions are mandatory to reproduce the trend of binding energies throughout these chains and to obtain a good description of two-neutron separation energies. At the same time, nuclei in this mass region are systematically overbound by about 40 MeV and the $N = 20$ magic gap is significantly overestimated. The present results show that ab initio many-body calculations can now access entire medium-mass isotope chains and provide a critical testing ground for modern theories of nuclear interactions.

PACS numbers: 21.60.De, 21.30.-x, 21.45.Ff, 27.40.+z

Introduction. Many-body interactions involving more than two nucleons have been long known to play an important role in nuclear physics. They arise naturally, due to the internal structure of the nucleon and are deemed to be necessary to explain saturation properties of nucleonic matter [1–3]. In finite systems, three-nucleon forces (3NFs) provide key mechanisms that govern the shell evolution and the position of the driplines. Their explicit treatment is mandatory in ab initio approaches and is becoming routine in modern nuclear structure calculations. Studies based on interactions derived from chiral effective field theory (EFT) [4] have shown that leading two-pion 3NF terms (of the Fujita-Miyazawa type) induce changes in the location of traditional magic numbers and explain the anomalous position of the oxygen neutron dripline compared to neighbouring elements [5–7]. Microscopic shell model calculations based on chiral 3NFs have been performed for isotopes up to calcium [5, 8]. Yet, full-fledged ab initio approaches have been so far limited to isotopic chains in the oxygen mass region [6, 7, 9] and are being tested in heavier systems only for isolated closed-shell cases [10–12]. Here we present the first ab initio calculation of five complete isotopic chains around $Z = 20$, including several truly open-shell systems. This extends the systematic and model-independent description of nuclei beyond the light sector of the nuclear chart, opening up a new significant region in which chiral interactions can be probed.

Ab initio many-body methods currently capable of targeting the calcium region include self-consistent Green's function (SCGF) [7, 13], coupled cluster [14, 15] and in-medium similarity renormalisation group (IM-SRG) [10, 16] theories. Such approaches make use of sophisticated and accurate many-body schemes that however have been restricted, until not long ago, to the vicinity of doubly-magic systems. To

overcome this limitation, some of the authors have recently introduced a new method based on the Gorkov reformulation of SCGF theory [17] and produced proof-of-principle calculations [18, 19] up to ^{74}Ni . The present work constitutes the first application of such Gorkov-Green's function (GGF) technique with a realistic Hamiltonian. In particular, the effect of state-of-the-art chiral 3N interactions in mid-mass nuclei is analyzed. We discuss results for absolute binding energies of Ar, K, Ca, Sc and Ti and show that employed chiral forces systematically overbind nuclei in the Ca region, in contrast to what was seen around oxygen [6, 7]. On the other hand, when leading 3NFs are incorporated, relative energies (specifically two-neutron separation energies) are fairly well reproduced.

Formalism. We start from the intrinsic Hamiltonian $\hat{H}_{int} = \hat{T} - \hat{T}_{cm} + \hat{V} + \hat{W}$, with the kinetic energy of the center of mass subtracted and \hat{V} and \hat{W} the two-nucleon (NN) and 3N interactions. The Gorkov formalism exploits the breaking of particle-number symmetry to effectively account for the non-perturbative physics associated with pairing correlations. Specifically, it targets the ground state, $|\Psi_0\rangle$, of the grand canonical Hamiltonian $\hat{\Omega}_{int} = \hat{H}_{int} - \mu_p \hat{Z} - \mu_n \hat{N}$ under the constraint that the correct particle number $A = N + Z$ is recovered on average: $Z = \langle \Psi_0 | \hat{Z} | \Psi_0 \rangle$ and $N = \langle \Psi_0 | \hat{N} | \Psi_0 \rangle$. The many-body Schrödinger equation is transformed into the Gorkov equation,

$$\begin{pmatrix} T + \Sigma^{11}(\omega) - \mu_k & \Sigma^{12}(\omega) \\ \Sigma^{21}(\omega) & -T + \Sigma^{22}(\omega) + \mu_k \end{pmatrix} \Big|_{\omega_k} \begin{pmatrix} \mathcal{U}^k \\ \mathcal{V}^k \end{pmatrix} = \omega_k \begin{pmatrix} \mathcal{U}^k \\ \mathcal{V}^k \end{pmatrix}, \quad (1)$$

whose solutions are the poles of the single-nucleon propagators, $\omega_k \equiv \Omega_k - \Omega_0$, where the index k refers to normalized eigenstates of $\hat{\Omega}_{int}$ that fulfill $\hat{\Omega}_{int} |\Psi_k\rangle = \Omega_k |\Psi_k\rangle$, and the probability amplitudes \mathcal{U}^k (\mathcal{V}^k) to reach state $|\Psi_k\rangle$ by adding (removing) a nucleon to (from) $|\Psi_0\rangle$. The self-energy

splits into static (first order) and dynamic terms, $\Sigma(\omega) = \Sigma^{(\infty)} + \Sigma^{(dyn)}(\omega)$. In the present work we consider all first- and second-order contributions, which define the many-body truncation of the method.

The inclusion of 3NFs in standard SCGF formalism is discussed in depth in [20], with first applications in Refs. [1, 7, 20]. Here we modify the prescription of Ref. [7] to extend the new Gorkov GF approach [17, 19] to 3NFs for the first time. The second-order self-energy contains solely interaction-irreducible diagrams and it is calculated using only an effective NN interaction, which includes contributions from \hat{W} . However, the static self-energy acquires extra terms from interaction-reducible diagrams involving 3NFs. Hence, we calculate $\Sigma^{(\infty)}$ as usual in terms of the NN interaction, \hat{V} , and then add the following 3NFs corrections:

$$\Delta\Sigma_{\alpha\beta}^{11,(\infty)} = - \left[\Delta\Sigma_{\bar{\alpha}\bar{\beta}}^{22,(\infty)} \right]^* = \frac{1}{2} \sum_{\gamma\delta\mu\nu} W_{\alpha\gamma\delta,\beta\mu\nu} \rho_{\mu\gamma} \rho_{\nu\delta}, \quad (2a)$$

$$\Delta\Sigma_{\alpha\beta}^{12,(\infty)} = \left[\Delta\Sigma_{\beta\alpha}^{21,(\infty)} \right]^* = \frac{1}{2} \sum_{\gamma\delta\mu\nu} W_{\alpha\bar{\beta}\delta,\mu\bar{\nu}\gamma} \bar{\rho}_{\mu\nu} \rho_{\gamma\delta}, \quad (2b)$$

where greek indices α, β, \dots label a complete orthonormal single-particle basis (barred quantities refer to time-reversed states) and ρ ($\bar{\rho}$) denotes the normal (anomalous) one-body density matrix [17].

Our calculations follow the sc0 approximation that is introduced in Ref. [19] and start by solving the Hatree-Fock-Bogoliubov equation within the chosen single-particle model space, including 3NFs in full. This provides the reference state and the corresponding density matrices that are used to generate the effective NN interaction according to Refs. [7, 20]. Following the sc0 prescription, $\Sigma^{(dyn)}$ remains unchanged throughout the rest of the calculation while $\Sigma^{(\infty)}$ is evaluated in a self-consistent fashion in terms of correlated density matrices. As discussed in Ref. [19], this procedure represents the optimal compromise between accuracy and computational cost and was found to be accurate to 1% or better.

Once convergence is reached, the total energy is calculated through the Koltun sum rule corrected for the presence of 3NFs [7, 20],

$$E_0^A = E_0^{A(NN)} - \frac{1}{2} \langle \Psi_0 | \hat{W} | \Psi_0 \rangle, \quad (3)$$

where $E_0^{A(NN)}$ represents the energy sum rule for NN interactions only, adapted to the Gorkov framework [17]. The expectation value of \hat{W} is obtained at first order in terms of the *correlated* normal density matrix

$$\langle \Psi_0 | \hat{W} | \Psi_0 \rangle \approx \frac{1}{6} \sum_{\alpha\beta\gamma\mu\nu\xi} W_{\alpha\beta\gamma,\mu\nu\xi} \rho_{\mu\alpha} \rho_{\nu\beta} \rho_{\xi\gamma}. \quad (4)$$

The contribution containing two anomalous density matrices was checked to be negligible and hence is not included here.

The present formalism assumes a $J^\Pi = 0^+$ ground state and therefore targets even-even systems. The ground state energy

of odd-even neighbours is obtained through [17, 21]

$$E_0^A = \bar{E}^A + \omega_{k=0}, \quad \text{for } A \text{ odd}, \quad (5)$$

where \bar{E}^A is the energy of the odd-even nucleus computed as if it were an even-even one, i.e. as a fully paired even number-parity state but forced to have an odd number of particles on average, while $\omega_{k=0}$ denotes the lowest pole energy extracted from Eq. (1) for that calculation. Eq. (5) is potentially exact such that its ability to account for blocking and polarization effects (and beyond) only depends on the scheme used to truncate the self-energy expansion.

Results. Calculations were performed using chiral NN and 3N forces evolved to low momentum scales through free-space similarity renormalization group (SRG) techniques [22]. The original NN interaction is generated at next-to-next-to-next-to-leading order (N³LO) with cutoff $\Lambda_{2N}=500$ MeV [23, 24], while a local N²LO 3NF [25] with a reduced cutoff of $\Lambda_{3N}=400$ MeV is employed. The 3NF low-energy constants $c_D=-0.2$ and $c_E=0.098$ are fitted to reproduce ⁴He binding energy [15]. The SRG evolution on the sole chiral NN interaction already generates 3N operators in the Hamiltonian, which we refer hereafter to as the “induced” 3NF. When the pre-existing chiral 3N interaction, including the two-pion exchange Fujita-Miyazawa contribution, is included, we refer to the “full” 3NF. Calculations were performed in model spaces up to 14 harmonic oscillator (HO) shells [$N_{max} \equiv \max(2n+l) = 13$], including all NN matrix elements and limiting 3NF ones to configurations with $N_1+N_2+N_3 \leq N_{max}^{3NF}=16$. An SRG cutoff $\lambda=2.0$ fm⁻¹ and HO frequency $\hbar\Omega=28$ MeV were used.

Figure 1 shows the ⁵¹K binding energy as a function of the model space size and the HO frequency used. Being one of the heaviest nuclei considered here, ⁵¹K is representative of the slowest convergence obtained in this work. Changing the model space from $N_{max}=12$ to 13 lowers its ground-state energy by 2.1 MeV, which corresponds to about 0.5% of the total binding energy. This is much smaller than the uncertainties resulting from truncating the many-body expansion of the self-energy at second order (see below). Other isotopes have similar speeds of convergence. For example, the change

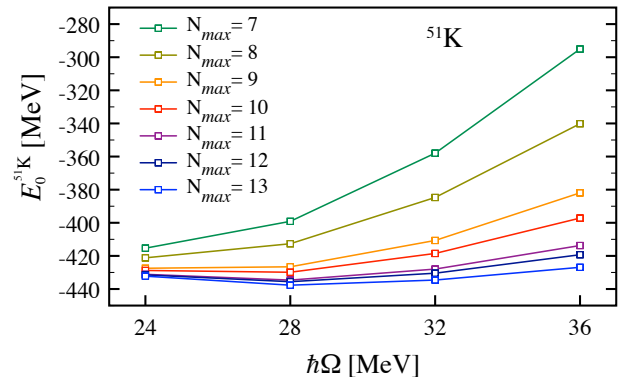


FIG. 1. (Color online) Convergence of the binding energy of ⁵¹K with respect to the basis size and HO frequency, for the full Hamiltonian.

for the same variation of the model space induces a change of 1.7 MeV for ^{49}K which slowly decreases to about 1 MeV in ^{40}Ca . Thus, one expects convergence errors to cancel to a large extent when calculating two-neutron separation energies $S_{2n} \equiv E_0^A - E_0^{A-2}$, where the change in A is for the removal of two neutrons. To test this we performed exponential extrapolations of the calculated binding energies of a few nuclei, using the last few odd values of N_{max} . We found variations of at most ≈ 500 keV with respect to the value calculated at $N_{max}=13$. Hence, we take this as an estimate of the convergence error on computed S_{2n} . In the following we present our results calculated for $N_{max}=13$ and $\hbar\Omega=28$ MeV, which corresponds to the minimum of the curve in Fig. 1. For isotopes beyond $N=32$, appropriate extrapolations and larger model spaces are required and will be considered in future works.

The accuracy of the many-body truncation of the self-energy at second order must also be assessed. To this extent, we consider the standard formulation of SCGF, based on the Dyson equation, which has been implemented with the third order algebraic diagrammatic construction [ADC(3)], which includes all third order diagrams and resums higher-orders non-perturbatively [26, 27]. We compute closed-shell isotopes ^{40}Ca , ^{48}Ca and ^{52}Ca for which Dyson ADC(3) calculations with $N_{max}=9$ can be performed and compared to second order Gorkov calculations (Gorkov-GF theory intrinsically reduces to Dyson-GF theory in closed-shell systems). Results in the top panel of Fig. 2 show that the correction from third- and higher-order diagrams is similar in the three isotopes. Specifically, we obtain $E_0^{ADC(3)-Dys} - E_0^{2nd-Gkv} = -10.6, -12.1$ and -12.6 MeV that correspond to $\approx 2.7\%$ of the total binding energy. Assuming that these differences are converged with respect to the model space, we add them to our second order Gorkov results with $N_{max}=13$ and display the results in the bottom panel of Fig. 2. Resulting values agree well with IM-SRG calculations of ^{40}Ca and ^{48}Ca based on the same Hamiltonian [10]. This confirms the robustness of the present results across different many-body methods. The error due to missing induced 4NFs was also estimated in Ref. [10] by varying the SRG cutoff over a (limited) range. Up to $\approx 1\%$ variations were found for masses $A \leq 56$ (e.g. less than 0.5% for ^{40}Ca and ^{48}Ca) when changing λ between 1.88 and 2.24 fm^{-1} . We take this estimate to be generally valid for all the present results.

A first important result of this Letter appears in the bottom panel of Fig. 2, which compares the results obtained with NN plus induced and NN plus full 3NFs. The trend of the binding energy of Ca isotopes is predicted incorrectly by the induced 3NF alone. This is fully amended by the inclusion of leading chiral 3NFs. However, the latter introduce additional attraction that results in a systematic overbinding of ground-state energies throughout the whole chain. Analogous results are obtained for Ar, K, Sc and Ti isotopic chains (not shown here), leading to the same conclusion regarding the role of the initial chiral 3NF in providing the correct trend and in generating overbinding at the same time.

The NN plus induced 3N interaction, which originates from the NN-only $N^3\text{LO}$ potential, generates a wrong slope in

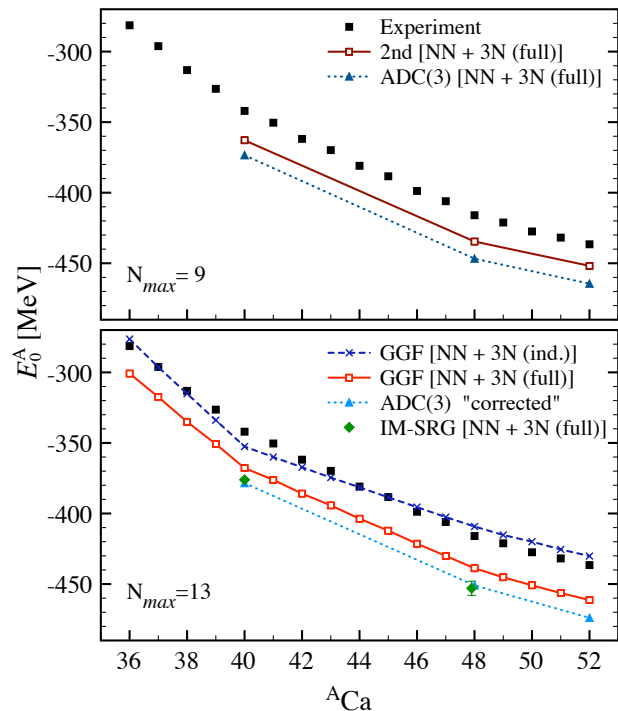


FIG. 2. (Color online) Experimental (full squares) [28–30] and calculated ground-state energies of Ca isotopes. *Top panel*: second-order Gorkov and Dyson-ADC(3) results for $^{40,48,52}\text{Ca}$ obtained with a $N_{max}=9$ model space and the full Hamiltonian. *Bottom panel*: second-order Gorkov results with NN plus induced (crosses) and NN plus full (open squares) 3NFs and $N_{max}=13$. Full 3NF Gorkov results corrected for the ADC(3) correlation energy extracted from the top panel (dotted line with full triangles). IM-SRG results [10] are for the same 3NF and are extrapolated to infinite model space (diamonds with error bars).

Fig. 2 and exaggerates the kink at ^{40}Ca . The corresponding two-nucleon separation energies are shown in Fig. 3 and are significantly too large (small) for $N \leq 20$ ($N > 20$). Including chiral 3NFs correct this behaviour to a large extent and predict S_{2n} close to the experiment for isotopes above ^{42}Ca . Figure 3 also shows results for microscopic shell model [8, 30] and coupled cluster [14] calculations above ^{41}Ca and ^{49}Ca , respectively, which are based on similar chiral forces. Our calculations confirm and extend these results within a full-fledged ab initio approach for the first time. The results are quite remarkable, considering that NN+3N chiral interactions have been fitted solely to few-body data up to $A = 4$.

The S_{2n} jump between $N=20$ and $N=22$ is largely overestimated with the NN plus induced 3NFs, which confirms the findings of Refs. [13, 31] based on the original NN interaction. The experimental $Z=20$ magic gap across ^{48}Ca is $\Delta_\pi(^{48}\text{Ca}) \equiv 2E_0^{48}\text{Ca} - E_0^{49}\text{Sc} - E_0^{47}\text{K} = 6.2$ MeV, whereas it was found to be 10.5 MeV in Ref. [31]. The magic gap is somewhat larger in the present calculations, i.e. it is equal to 16.5 MeV with the NN plus induced 3NF and is reduced to 12.4 MeV including the full 3NF, which still overestimates

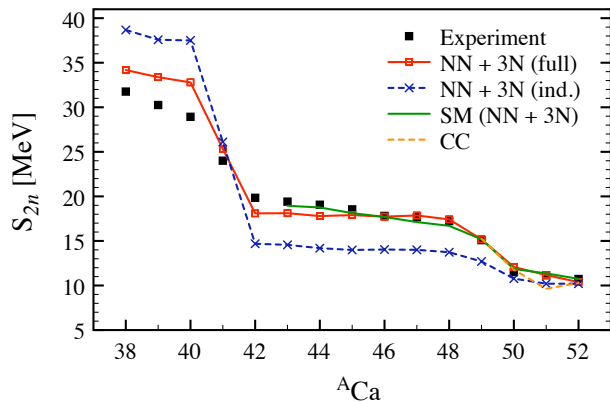


FIG. 3. (Color online) Two-nucleon separation energies, S_{2n} , of Ca isotopes. Gorkov calculations are shown for the induced (crosses) and full (open squares) Hamiltonians and are compared to the experiment (full squares) [28–30]. Results from shell model calculations with chiral 3NFs (full line) [8, 30] and coupled cluster (dashed line) [14] are also shown.

experiment by about 6 MeV.

The Koltun sum rule (3) computes the binding energy as a weighted sum of one-nucleon removal energies. The systematic overbinding observed in the present results thus relates to a spectrum in the A-1 system (not shown here) that is too spread out. This has already been seen in Ref. [13] and is reflected in the excessive distance between major nuclear shells, or effective single-particle energies (ESPE) [17, 32]. In turn, the overestimated N=20 magic gap and the jump of the S_{2n} between N=20 and N=22 relate to the exaggerated energy separation between *sd* and *pf* major shells generated by presently employed chiral interactions. Eventually, a too dilute ESPE spectrum translates into underestimated radii.

Presently, ADC(3)-corrected energies with the NN plus full 3NF (Fig. 2) overbind ^{40}Ca , ^{48}Ca and ^{52}Ca by 0.90, 0.73, and 0.72 MeV/A, respectively. It can be conjectured that such a behaviour correlates with a predicted saturation point of symmetric nuclear matter that is too bound and located at too high density compared to the empirical point. Recent calculations of homogeneous nuclear matter based on chiral interactions [2, 3] predict a saturation point in the vicinity of the empirical point with an uncertainty that is compatible with the misplacement suggested by our analysis. However, such calculations use a different 3NF cutoff $\Lambda_{3N}=500$ MeV and different values of c_D and c_E . Additional SCGF calculations as in Ref. [3] but with the same NN+3N chiral interactions used here would help in confirming this conjecture.

The systematic of S_{2n} obtained with the NN plus full 3NF is displayed in Fig. 4 along Ar, K, Ca, Sc and Ti isotopic chains, up to N=32. When the neutron chemical potential lies within the *pf* shell, predicted S_{2n} reproduce experiment to good accuracy without adjusting any parameter beyond $A = 4$ data. Still, the quality slightly deteriorates as the proton chemical potential moves down into the *sd* shell, i.e. going from Ca to K and Ar elements. The increasing underestimation of the S_{2n} is

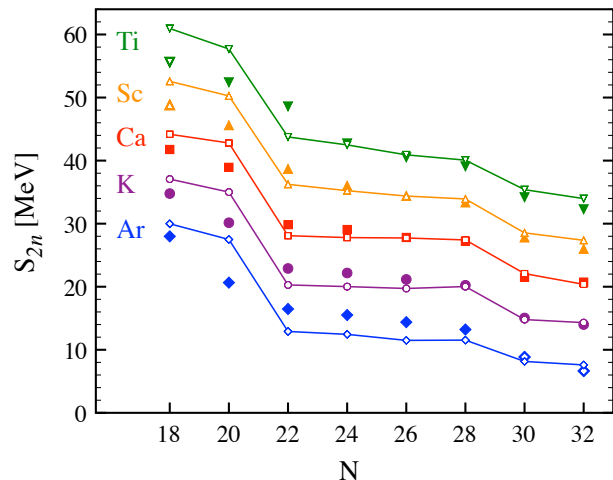


FIG. 4. (Color online) Two-neutron separation energies, S_{2n} , along Ar, K, Ca, Sc and Ti isotopic chains. The experimental values (solid symbols) [28–30] are compared to second-order Gorkov calculations with the NN plus full 3NF (full lines). Values for K, Ca, Sc and Ti are respectively shifted by +5 MeV, 10 MeV, 15 MeV and 20 MeV for display purposes. Isolated open symbols are AME2012 extrapolations of experimental data [28].

consistent with a too large gap between proton *sd* and *pf* major shells that prevents quadrupole neutron-proton correlations to switch on. The too large jump of the S_{2n} between N=20 and N=22 is visible for all elements and becomes particularly pronounced as one moves away from the proton magic ^{40}Ca nucleus where the experimental jump is progressively washed out. At N=18, the situation deteriorates when going from ^{38}Ca to ^{41}Sc and ^{42}Ti (but not going to ^{37}K and ^{36}Ar), i.e. when the proton chemical potential moves up into the *pf* shell. This is again consistent with an exaggerated shell gap between *sd* *pf* shells that prevents neutron-proton correlations to switch on when the chemical potentials sit on both sides of the gap. One should also notice that present calculations are restricted to densities with spherical symmetry and effects of deformation might play a role in some Ar or Ti isotopes. However, such effects will be minor in the S_{2n} and we do not expect the accurate treatment of deformation to alter any of our conclusions.

Conclusions. We have reported on the first application of the Gorkov-Green’s function approach with two- and three-body forces. We have shown that the present ab initio technique allows for the systematic description of mid-mass open-shell nuclei, including odd-even systems. This represents a qualitative breakthrough that opens up unprecedented possibilities in terms of nuclei reachable from an ab initio standpoint. Exploiting the mechanism of symmetry breaking and keeping the simplicity of a single-reference scheme, Gorkov’s framework could be naturally incorporated into other many-body approaches. Its applicability is not limited to nuclear physics but can be generally extended to many-body systems that present a near-degeneracies.

In this Letter we have focused on the ability of leading chi-

ral 3NFs to describe absolute binding and two-neutron separation energies along Ar, K, Ca, Sc and Ti chains, up to $N=32$. While available $NN+3N$ chiral interactions typically perform well in the vicinity of oxygen isotopes, they were never tested for entire isotopic chains with $Z > 9$. Leading 3NFs are found to be mandatory to reproduce the correct trend of binding energies for all isotopes, analogously to what was observed in lighter N, O and F chains. Overall, the systematic of two-neutron separation energies is reproduced with a very good quality. Still, absolute binding energies are systematically overestimated throughout the $Z \approx 20$ mass region and the magic character of $N=20$ and/or $Z=20$ nuclei is exaggerated by the employed $NN+3N$ chiral forces. This can be traced back to the fact that the latter make deeply bound effective single-nucleon shells too spread out and the distance between major shells too pronounced. It is conjectured that this relates to a saturation point of symmetric nuclear matter located at a slightly too large binding energy/density compared to the empirical point. Eventually, we conclude that ab initio many-body calculations of mid-mass isotopic chains can now challenge modern theories of elementary nuclear interactions.

Acknowledgements. This work was supported by the DFG through Grant No. SFB 634, by the Helmholtz Alliance Program, Contract No. HA216/EMMI, by the United Kingdom Science and Technology Facilities Council (STFC) under Grant ST/J000051/1 and by the Natural Sciences and Engineering Research Council of Canada (NSERC), Grant No. 401945-2011. TRIUMF receives funding via a contribution through the National Research Council Canada. Calculations were performed using HPC resources from GENCI-CCRT (Grant No. 2013-050707) and the DiRAC Data Analytic system at the University of Cambridge (BIS National E-infrastructure capital grant No. ST/K001590/1 and STFC grants No. ST/H008861/1, ST/H00887X/1, and ST/K00333X/1).

* vittorio.soma@physik.tu-darmstadt.de

† C.Barbieri@surrey.ac.uk

‡ thomas.duguet@cea.fr

- [1] V. Somà and P. Božek, *Phys. Rev. C* **78**, 054003 (2008).
- [2] K. Hebeler, S. K. Bogner, R. J. Furnstahl, A. Nogga, and A. Schwenk, *Phys. Rev. C* **83**, 031301 (2011).
- [3] A. Carbone, A. Polls, and A. Rios, *Phys. Rev. C* **88**, 044302 (2013).
- [4] E. Epelbaum, H.-W. Hammer, and U.-G. Meissner, *Rev. Mod. Phys.* **81**, 1773 (2009).
- [5] T. Otsuka, T. Suzuki, J. D. Holt, A. Schwenk, and Y. Akaishi, *Phys. Rev. Lett.* **105**, 032501 (2010).
- [6] H. Hergert, S. Binder, A. Calci, J. Langhammer, and R. Roth, *Phys. Rev. Lett.* **110**, 242501 (2013).
- [7] A. Cipollone, C. Barbieri, and P. Navrátil, *Phys. Rev. Lett.* **111**, 062501 (2013).
- [8] J. D. Holt, T. Otsuka, A. Schwenk, and T. Suzuki, *J. Phys.* **G39**, 085111 (2012).
- [9] T. A. Lähde, E. Epelbaum, H. Krebs, D. Lee, U.-G. Meiner, *et al.*, (2013), arXiv:1311.0477 [nucl-th].
- [10] H. Hergert, S. K. Bogner, S. Binder, A. Calci, J. Langhammer, R. Roth, and A. Schwenk, *Phys. Rev. C* **87**, 034307 (2013).
- [11] S. Binder, J. Langhammer, A. Calci, P. Navrátil, and R. Roth, *Phys. Rev. C* **87**, 021303 (2013).
- [12] S. Binder, J. Langhammer, A. Calci, and R. Roth, (2013), arXiv:1312.5685 [nucl-th].
- [13] C. Barbieri and M. Hjorth-Jensen, *Phys. Rev. C* **79**, 064313 (2009).
- [14] G. Hagen, M. Hjorth-Jensen, G. R. Jansen, R. Machleidt, and T. Papenbrock, *Phys. Rev. Lett.* **109**, 032502 (2012).
- [15] R. Roth, S. Binder, K. Vobig, A. Calci, J. Langhammer, and P. Navrátil, *Phys. Rev. Lett.* **109**, 052501 (2012).
- [16] K. Tsukiyama, S. K. Bogner, and A. Schwenk, *Phys. Rev. Lett.* **106**, 222502 (2011).
- [17] V. Somà, T. Duguet, and C. Barbieri, *Phys. Rev. C* **84**, 064317 (2011).
- [18] V. Somà, C. Barbieri, and T. Duguet, *Phys. Rev. C* **87**, 011303 (2013).
- [19] V. Somà, C. Barbieri, and T. Duguet, *Phys. Rev. C* **89**, 024323 (2014).
- [20] A. Carbone, A. Cipollone, C. Barbieri, A. Rios, and A. Polls, *Phys. Rev. C* **88**, 054326 (2013).
- [21] T. Duguet, P. Bonche, P. H. Heenen, and J. Meyer, *Phys. Rev. C* **65**, 014311 (2001).
- [22] E. D. Jurgenson, P. Navrátil, and R. J. Furnstahl, *Phys. Rev. Lett.* **103**, 082501 (2009).
- [23] D. R. Entem and R. Machleidt, *Phys. Rev. C* **68**, 041001 (2003).
- [24] R. Machleidt and D. R. Entem, *Phys. Rep.* **503**, 1 (2011).
- [25] P. Navrátil, *Few-Body Systems* **41**, 117 (2007).
- [26] J. Schirmer, L. S. Cederbaum, and O. Walter, *Phys. Rev. A* **28**, 1237 (1983).
- [27] C. Barbieri, D. Van Neck, and W. H. Dickhoff, *Phys. Rev. A* **76**, 052503 (2007).
- [28] M. Wang, G. Audi, A. Wapstra, F. Kondev, M. MacCormick, X. Xu, and B. Pfeiffer, *Chinese Physics C* **36**, 1603 (2012).
- [29] A. T. Gallant, J. C. Bale, T. Brunner, U. Chowdhury, S. Ettenauer, A. Lennarz, D. Robertson, V. V. Simon, A. Chaudhuri, J. D. Holt, A. A. Kwiatkowski, E. Mané, J. Menéndez, B. E. Schultz, M. C. Simon, C. Andreoiu, P. Delheij, M. R. Pearson, H. Savajols, A. Schwenk, and J. Dilling, *Phys. Rev. Lett.* **109**, 032506 (2012).
- [30] F. Wienholtz, D. Beck, K. Blaum, C. Borgmann, M. Breitenfeldt, *et al.*, *Nature* **498**, 346 (2013).
- [31] C. Barbieri, *Phys. Rev. Lett.* **103**, 202502 (2009).
- [32] T. Duguet and G. Hagen, *Phys. Rev. C* **85**, 034330 (2012).